

## High-throughput indentational elasticity measurements of hydrogel extracellular matrix substrates

Dexter J. D'Sa, Elena M. de Juan Pardo, Rosalia de las Rivas Astiz, Shamik Sen, and Sanjay Kumar

Citation: *Appl. Phys. Lett.* **95**, 063701 (2009); doi: 10.1063/1.3197013

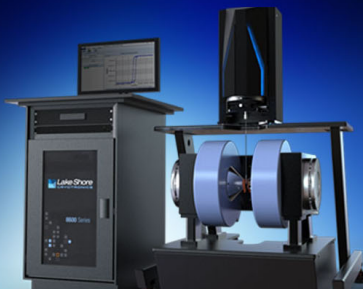
View online: <http://dx.doi.org/10.1063/1.3197013>

View Table of Contents: <http://aip.scitation.org/toc/apl/95/6>

Published by the [American Institute of Physics](#)

---

---



### NEW 8600 Series VSM

For fast, highly sensitive  
measurement performance

LEARN MORE 

## High-throughput indentational elasticity measurements of hydrogel extracellular matrix substrates

Dexter J. D'Sa, Elena M. de Juan Pardo,<sup>a)</sup> Rosalia de las Rivas Astiz,<sup>b)</sup> Shamik Sen, and Sanjay Kumar<sup>c)</sup>

*Department of Bioengineering, University of California, Berkeley, California 94720-1762, USA*

(Received 12 June 2009; accepted 9 July 2009; published online 10 August 2009)

Much interest surrounds the effect of extracellular matrix (ECM) elasticity on cell behavior. Here we present a rapid method for measuring the elasticity of synthetic ECM substrates based on indentation of the substrate with a ferromagnetic sphere and optical tracking of the resulting deformation. We find that this method yields order-of-magnitude agreement with atomic force microscopy elasticity measurements, but that the degree of this agreement depends strongly on sphere density and gel elasticity. In its regime of greatest accuracy, we envision that this method may be used for high-throughput characterization of ECM substrates in cell biological studies.

© 2009 American Institute of Physics. [DOI: 10.1063/1.3197013]

Over the past two decades, cell biologists have begun to recognize that cells are exquisitely sensitive to mechanical inputs from their surroundings, including the extracellular matrix (ECM) and the solid-state biopolymeric scaffold to which cells adhere in tissues. It has become especially clear that the elasticity (Young's modulus) of the ECM can powerfully regulate many cellular properties, including structure, adhesion, migration, proliferation, and death.<sup>1,2</sup> For stem and progenitor cells, ECM elasticity can guide self-renewal and differentiation into specific lineages,<sup>3,4</sup> and for tumor cells, it can guide the initial stages of tissue dysplasia<sup>5</sup> as well as later proliferation and invasion.<sup>6</sup>

This surge of interest in "cellular mechanobiology" has in turn given rise to material platforms that enable one to culture living cells on synthetic ECM substrates of precisely defined elasticity. Perhaps the most widely used of these platforms is based on synthesis and biofunctionalization of polyacrylamide (PA) hydrogels.<sup>7,8</sup> In this system, the elasticity is determined by the ratio of the monomer (acrylamide) to the crosslinker (bisacrylamide), and the cell adhesive function is derived by grafting full-length ECM proteins onto the surface at defined coverage. Meaningful interpretation of results from this system relies on accurate knowledge of the effective elasticity experienced by the cell at the hydrogel surface. Traditionally, this value has been inferred from bulk mechanical properties of the hydrogel, for example, as measured by macroscale extensional<sup>8</sup> or oscillatory<sup>6</sup> rheometry. While relatively high-throughput in practice, these measurements depend strongly on sample geometry, strain rate, and other experimental details. Moreover, cell-ECM interactions occur at interfaces and involve cellular mechanosensors and ECM proteins that are micro- and nanoscale in size, raising questions about the appropriateness of bulk approaches. Thus, atomic force microscopy (AFM) has gained favor for measuring ECM elasticity; here the AFM tip is used to indent the ECM surface, and the force versus indentation depth

profile is fit to an indentational model to extract the Young's modulus. However, AFM is skill-intensive, low-throughput, and requires expensive instrumentation. These limitations are particularly problematic if there are significant sample-to-sample variations in elasticity that necessitate serial measurement of every ECM substrate individually.

To address these issues, we developed a strategy for measuring the indentational elasticity of PA-based ECM hydrogels that combines the high-throughput nature of bulk rheometric methods and the microscale, interfacial nature of AFM (Fig. 1). Our strategy is based on embedding fluorescent fiduciary markers within the hydrogel, which we introduce prior to polymerization and gelation, and indentation of the PA surface with a microscale, ferromagnetic sphere of known density ( $\rho_{\text{sphere}}$ ) and radius ( $R_{\text{sphere}}$ ). Using a motorized imaging system that enables us to acquire epifluorescence and phase-contrast images at defined imaging planes in the vertical ( $z$ ) direction, we obtain  $z$ -stacks of the gel both at the horizontal ( $x$ - $y$ ) position of sphere indentation and another position far from the sphere. The former data enable us to determine the  $z$ -positions of the diameter of the sphere ( $z_{\text{sphere}}$ ); the latter data enable us to determine the plane of the unindented gel surface ( $z_{\text{gel}}$ ), which we define as the plane at which we first begin to detect in-focus fluorescence from the embedded markers. The indentation depth ( $\delta$ ) is then calculated as  $\delta = R_{\text{sphere}} - (z_{\text{sphere}} - z_{\text{gel}})$ , and gel elasticity ( $E$ ) is calculated using an equation for Hertzian indentation of a semi-infinite, linearly elastic material with an infinitely stiff spherical probe,<sup>9</sup> assuming the only forces acting on the sphere are gravity and fluid buoyancy:

$$E = \pi(1 - \nu_{\text{gel}}^2) \delta^{-3/2} R_{\text{sphere}}^{5/2} g (\rho_{\text{sphere}} - \rho_{\text{fluid}}). \quad (1)$$

Here,  $\rho_{\text{fluid}}$  is the density of the fluid,  $\nu_{\text{gel}}$  is the Poisson's ratio of the gel (0.3),<sup>10</sup> and  $g$  is the acceleration of gravity (9.8 m/s<sup>2</sup>). Importantly, this equation would need to be revised to include additional force terms for any material-sphere system that violates these assumptions, such as materials that strain-stiffen or are thin enough to transmit mechanical information from the underlying substrate, or spheres whose surface chemistry promotes or inhibits wetting by the gel surface.

<sup>a)</sup>Present address: TECNUN and CEIT, University of Navarra, San Sebastian, Spain.

<sup>b)</sup>Present address: Procter & Gamble Co., London, United Kingdom.

<sup>c)</sup>Author to whom correspondence should be addressed. Electronic mail: skumar@berkeley.edu. Tel.: 510-643-0787. FAX: 510-642-5835.

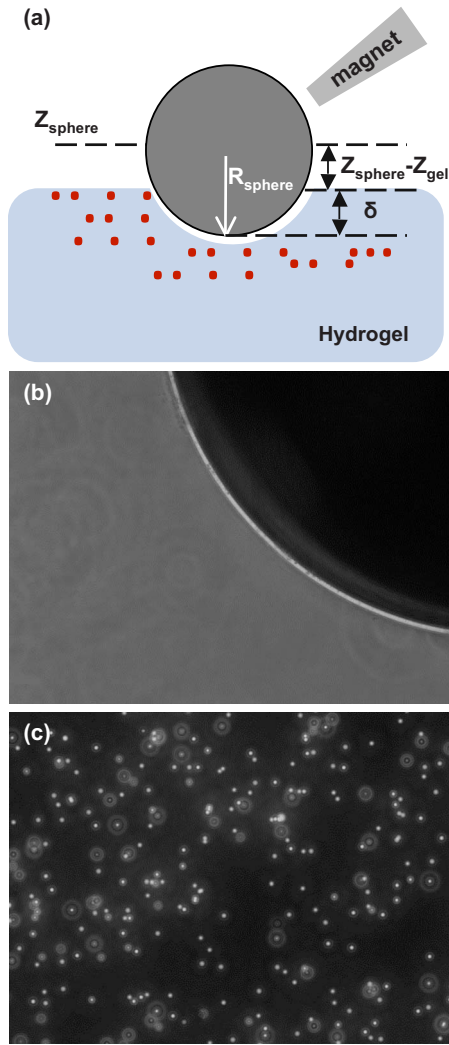


FIG. 1. (Color online) Indentation measurement. (a) Schematic of experiment and measured parameters. Prior to polymerization, fluorescent markers are embedded throughout the hydrogel, including near the surface. A ferromagnetic sphere is then deposited onto the gel using a switchable magnet (switched reluctance device) consisting of a sharp-tipped ferrite rod in separable contact with an NdFeB permanent magnet. This placement results in the deformation of the hydrogel, which displaces nearby embedded markers. Because the sphere is ferromagnetic, it may later be withdrawn from the surface (not shown). Key measured quantities include  $z_{\text{gel}}$  (plane of the free gel surface),  $z_{\text{sphere}}$  (plane of the diameter of the sphere), and  $R_{\text{sphere}}$  (radius of the sphere). The indentation depth ( $\delta$ ) is then calculated as  $\delta = R_{\text{sphere}} - (z_{\text{sphere}} - z_{\text{gel}})$ . (b) Phase contrast image at the focal plane of the equator of a sphere ( $z_{\text{sphere}}$ ) of nominal radius  $495 \mu\text{m}$ . (c) Epifluorescence image of the surface of the gel ( $z_{\text{gel}}$ ), showing fiduciary markers (nominal radii  $500 \text{ nm}$ ). Out-of-focus markers embedded deeper within the gel are also visible. Note that the magnification of (c) is twice as high as (b) to facilitate depiction of fiduciary markers.

We synthesized a series of hydrogels over a range of acrylamide: bisacrylamide ratios<sup>6</sup> and used our sphere indentation strategy to measure the elasticity of each gel. In order to compare these findings to a previously validated method, we also measured the elasticity of each gel with an Asylum MFP-3D AFM as previously described.<sup>11</sup> To examine possible contributions of sphere density to apparent elasticity, we obtained AFM and sphere indentation measurements for spheres of three different densities ( $15\,300$ ,  $26\,200$ , and  $151\,000 \text{ kg/m}^3$ ). When we compared the elasticities measured by the two methods, we found an order-of-magnitude agreement for all three spheres for  $E$  (as measured by AFM)

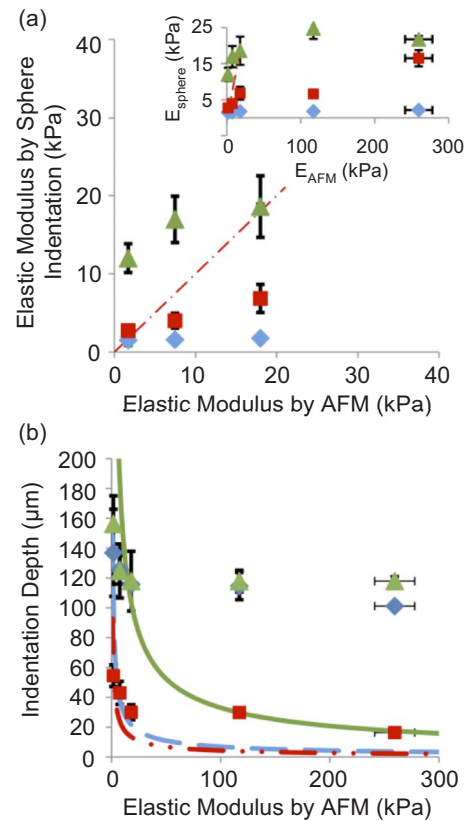


FIG. 2. (Color online) Comparison of sphere indentation method with AFM. Measurements were made with three spheres of varying density:  $151\,000 \text{ kg/m}^3$  (triangles),  $26\,200 \text{ kg/m}^3$  (squares), and  $15\,300 \text{ kg/m}^3$  (diamonds). (a) Direct comparison of elastic moduli measured by AFM and by sphere indentation. The dotted line represents a perfect match between the two methods of measurement. For  $E > 20 \text{ kPa}$  the sphere indentation method significantly underpredicts the elastic modulus obtained by AFM (inset). The data symbols in the inset match those in the main figure, and the dashed line again represents a slope of 1. (b) Comparison of measured and theoretical indentation-stiffness ( $\delta$  vs  $E$ ) relationships. Individual markers represent experimentally obtained indentation depths. The solid, dashed, and dashed/dotted lines represent the indentation depth ( $\delta$ ) vs AFM-measured gel elasticity ( $E$ ) curves predicted from Eq. (1) for the  $151\,000 \text{ kg/m}^3$  sphere, the  $26\,200 \text{ kg/m}^3$  sphere, and the  $15\,300 \text{ kg/m}^3$  sphere, respectively. Error bars in  $x$  and  $y$  represent mean  $\pm$  SD.

$< 20 \text{ kPa}$  [Fig. 2(a)]. Specifically, the most and least dense spheres ( $151\,000 \text{ kg/m}^3$  and  $15\,300 \text{ kg/m}^3$ ) produced the greatest agreement with AFM ( $> 90\%$ ) for high and low values of  $E$ , respectively. Interestingly, for  $E > 20 \text{ kPa}$ , all three spheres drastically underpredicted the value measured by AFM [Fig. 2(a), inset], with the least dense sphere yielding the greatest underprediction.

To gain additional insight, we compared the measured indentation depth of each sphere on each gel against the elasticity of that gel as measured by AFM, and we superimposed the theoretical  $\delta$ -versus- $E$  relationship predicted for each sphere by Eq. (1) [Fig. 2(b)]. This representation revealed that for  $E > 100 \text{ kPa}$ , all three spheres indented more deeply than expected and displayed saturation behavior, with indentation depths falling with increasing  $E$  as expected but reaching a plateau value on the stiffest gels. The origins of these effects are unclear and may be due to our reduced ability to measure the small indentations on the stiffest substrates, variations in gel topography, or sphere-gel interfacial interactions and contact area at high stiffness. In particular, wetting of the sphere by the gel surface would be consistent with

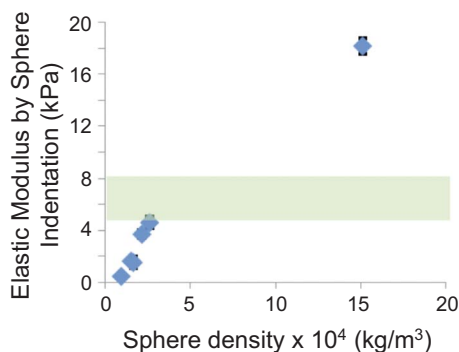


FIG. 3. (Color online) Influence of  $\rho_{\text{sphere}}$  on  $E$  for a single gel of defined stiffness (5–8 kPa) for five spheres of varying density (see Table I). The horizontal shaded band represents  $E$  (mean  $\pm$  SD) as measured by AFM. Error bars represent mean  $\pm$  SD, and data reflects multiple, independent sphere indentation measurements ( $N=3$ ) on multiple, independent hydrogel samples ( $N=3$ ).

a saturation relationship and create significant deviations from our Hertzian indentation model. Systematic manipulation of sphere-gel surface chemistry together with higher-resolution imaging would help evaluate this further.

To continue exploring the relationship between sphere density and measured elasticity, we repeated our measurements with three additional spheres whose densities fall within the range of 9550–26 200 kg/m<sup>3</sup> (i.e., the low-density regime) on a relatively compliant gel of  $E \sim 5$ –8 kPa by AFM (Fig. 3 and Table I). While all of these additional spheres yielded accurate order-of-magnitude measurements, they also underpredicted the AFM-measured elasticity, and did so in a strongly density-dependent manner. While all spheres came within an order of magnitude of agreeing with AFM, the intermediate-density spheres matched most closely, a finding that further the notion that the accuracy of this method depends dramatically on sphere density. We hypothesize that the increased effective elasticity experienced by the densest spheres may be due to mechanical contributions from the rigid underlying glass substrate, which would be expected to play an increasingly significant role at the high indentations made by these spheres.<sup>12</sup>

There have been at least two other published reports of extraction of PA gel elastic moduli from sphere indentation measurements.<sup>7,13</sup> These studies infer indentation depths by measuring  $z$  positions of embedded fluorescent fiducial markers before and after removing the sphere from the surface, which can be difficult to accurately track and localize and require the use of sophisticated marker selection

TABLE I. Table of spheres used in this study, including radius and density. In all cases, sphere radii were measured using micrometer calipers and densities were calculated by dividing the measured mass by the spherical volume predicted from the radius measurement.

Sphere density kg/m <sup>3</sup>	Sphere radius ( $\mu\text{m}$ )
9550	396.88
153 000	495.30
16 600	496.06
21 700	297.69
26 200	297.69
151 000	495.30

software.<sup>13</sup> The act of removing the sphere also sometimes damages the gel, complicating marker tracking. These studies also do not offer generalized expressions that explicitly incorporate the buoyancy of the sphere, which may vary with media conditions and strongly influences measurement accuracy. Most importantly, our study takes the critical step of comparing sphere indentation measurements to AFM over a range of gel formulations and sphere densities. Our data highlight the importance of choosing an appropriate-density sphere for a given gel elasticity and comparing results with standard rheological methods.

We envision two potential uses for this method. First, the range of greatest accuracy of this method ( $E < 20$  kPa) encompasses the elasticities of all but the most rigid biological tissues,<sup>14</sup> making this approach useful for measuring elasticities of many tissue-mimetic ECMs. Second, this method could be used for order-of-magnitude quality control in applications that require fabrication of many hydrogel ECMs, e.g., for harvesting cellular proteins for biochemical analysis or for mechanically stimulating cell cultures through application of static or cyclic strains. Because the spheres may be magnetically deposited and withdrawn, and because the measurement of indentation depth comes entirely from optical imaging of the substrate, this method lends itself to parallelization and automation in ways that AFM does not. Thus, its utility may extend beyond characterization of hydrogel ECMs for cell culture to any linearly elastic material. Additional studies should reveal whether the general principles and regimes of greatest accuracy revealed here for PA hold for other material systems.

This work was supported by the Arnold and Mabel Beckman Young Investigator Award and the NIH Director's New Innovator Award (1DP2OD004213), a part of the NIH Roadmap for Biomedical Research (both to S.K.). R.R.A. gratefully acknowledges support from the Fundación Rafael Escolá. We thank Professor S. Conolly for his generous provision of the ferromagnets, critical design input on the switched reluctance device, and valuable feedback on the manuscript.

<sup>1</sup>D. E. Discher, P. Janmey, and Y. L. Wang, *Science* **310**, 1139 (2005).

<sup>2</sup>Y. W. Lin, C. M. Cheng, P. R. Leduc, and C. C. Chen, *PLoS ONE* **4**, e4293 (2009).

<sup>3</sup>A. J. Engler, S. Sen, H. L. Sweeney, and D. E. Discher, *Cell* **126**, 677 (2006).

<sup>4</sup>K. Saha, A. J. Keung, E. F. Irwin, Y. Li, L. Little, D. V. Schaffer, and K. E. Healy, *Biophys. J.* **95**, 4426 (2008).

<sup>5</sup>M. J. Paszek, N. Zahir, K. R. Johnson, J. N. Lakins, G. I. Rozenberg, A. Gefen, C. A. Reinhart-King, S. S. Margulies, M. Dembo, D. Boettiger, D. A. Hammer, and V. M. Weaver, *Cancer Cell* **8**, 241 (2005).

<sup>6</sup>T. A. Ulrich, E. M. de Juan Pardo, and S. Kumar, *Cancer Res.* **69**, 4167 (2009).

<sup>7</sup>C. M. Lo, H. B. Wang, M. Dembo, and Y. L. Wang, *Biophys. J.* **79**, 144 (2000).

<sup>8</sup>R. J. Pelham, Jr. and Y. Wang, *Proc. Natl. Acad. Sci. U.S.A.* **94**, 13661 (1997).

<sup>9</sup>W. F. Heinz and J. H. Hoh, *Trends Biotechnol.* **17**, 143 (1999).

<sup>10</sup>Y. Li, Z. Hu, and C. Li, *J. Appl. Polym. Sci.* **50**, 1107 (1993).

<sup>11</sup>S. Sen and S. Kumar, *Cell. Mol. Bioeng.* **2**, 218 (2009).

<sup>12</sup>A. J. Engler, L. Richart, J. Y. Wong, C. Picart, and D. E. Discher, *Surf. Sci.* **570**, 142 (2004).

<sup>13</sup>V. Damljanovic, B. C. Lagerholm, and K. Jacobson, *BioTechniques* **39**, 847 (2005).

<sup>14</sup>A. J. Keung, K. E. Healy, S. Kumar, and D. V. Schaffer, *WIREs Syst. Biol. Med.* (to be published), doi: 10.1002/wsbm.46.